HHS Public Access

Author manuscript

J Thromb Haemost. Author manuscript; available in PMC 2024 May 01.

Published in final edited form as:

J Thromb Haemost. 2023 May ; 21(5): 1366–1380. doi:10.1016/j.jtha.2023.01.027.

JAK-STAT inhibition reduces endothelial prothrombotic activation and leukocyte–endothelial proadhesive interactions

Joan D. Beckman[1], **Angelica DaSilva**[2], **Elena Aronovich**[1], **Aithanh Nguyen**[1], **Julia Nguyen**[1], **Geneva Hargis**[2], **David Reynolds**[3], **Gregory M. Vercellotti**[1], **Brian Betts**[1], **David K. Wood**[2]

[1]Department of Medicine, Division of Hematology, Oncology and Transplantation, University of Minnesota, Minneapolis, Minnesota, USA

[2]Department of Biomedical Engineering, University of Minnesota, Minneapolis, Minnesota, USA

[3]Department of Biomedical Engineering, University of Pennsylvania, Philadelphia, Pennsylvania, USA

Abstract

Background: Vascular activation is characterized by increased proinflammatory, pro thrombotic, and proadhesive signaling. Several chronic and acute conditions, including *Bcr-abl*-negative myeloproliferative neoplasms (MPNs), graft-vs-host disease, and COVID-19 have been noted to have increased activation of the janus kinase (JAK)-signal transducer and downstream activator of transcription (STAT) pathways. Two notable inhibitors of the JAK-STAT pathway are ruxolitinib (JAK1/2 inhibitor) and fedratinib (JAK2 inhibitor), which are currently used to treat MPN patients. However, in some conditions, it has been noted that JAK inhibitors can increase the risk of thromboembolic complications.

Objectives: We sought to define the anti-inflammatory and antithrombotic effects of JAK-STAT inhibitors in vascular endothelial cells.

Methods: We assessed endothelial activation in the presence or absence of ruxolitinib or fedratinib by using immunoblots, immunofluorescence, qRT-PCR, and function coagulation assays. Finally, we used endothelialized microfluidics perfused with blood from normal and *JAK2*$^{V617F+}$ individuals to evaluate whether ruxolitinib and fedratinib changed cell adhesion.

Results: We found that both ruxolitinib and fedratinib reduced endothelial cell phospho-STAT1 and STAT3 signaling and attenuated nuclear phospho-NK-κB and phospho-c-Jun localization. JAK-STAT inhibition also limited secretion of proadhesive and procoagulant P-selectin and von

Correspondence Joan D. Beckman, 420 Delaware St. SE, MMC 480, Minneapolis, Minnesota 55455 USA. beckm092@umn.edu.
TWITTER *Joan D. Beckman* @jd_beckman

AUTHOR CONTRIBUTIONS

J.D.B. designed and performed experiments, analyzed data, and wrote the manuscript. A.D.S. designed and performed experiments, analyzed data, and edited the manuscript. E.A. performed experiments, analyzed data, and edited the manuscript. A.N. and J.N. performed experiments and analyzed data. G.H. and D.R. designed and performed experiments and analyzed data. G.M.V., B.C.B., and D.K.W. designed experiments and edited the manuscript.

Remaining authors have no conflicts to disclose.

SUPPLEMENTARY MATERIAL

The online version contains supplementary material available at https://doi.org/10.1016/j.jtha.2023.01.027

Willebrand factor and proinflammatory IL-6. Likewise, we found that JAK-STAT inhibition reduced endothelial tissue factor and urokinase plasminogen activator expression and activity.

Conclusions: By using endothelialized microfluidics perfused with whole blood samples, we demonstrated that endothelial treatment with JAK-STAT inhibitors prevented rolling of both healthy control and *JAK2*^{V617F} MPN leukocytes. Together, these findings demonstrate that JAK-STAT inhibitors reduce the upregulation of critical prothrombotic pathways and prevent increased leukocyte-endothelial adhesion.

Keywords

endothelium; janus kinase inhibitors; tissue factor; thrombosis; myeloproliferative neoplasm

1 | INTRODUCTION

The janus kinase (JAK)-signal transducer and activator of transcription (STAT) pathway plays critical roles in orchestrating proinflammatory signaling pathways [1]. Binding of a ligand, such as erythropoietin or tumor necrosis factor (TNF), to a type I or II cytokine receptor [1] leads to a distinct JAK phosphorylation cascade that activates STATs [1]. However, in pathologic states, such as *Bcl-abl*-negative myeloproliferative neoplasms (MPNs), a *JAK2*^{V61F} point mutation permits ligand-independent JAK-STAT signaling, which in hematopoietic cells leads to an excess production of white blood cells, red blood cells, and platelets. Phenotypically, the *JAK2*^{V617F} mutation manifests as polycythemia vera (PV), essential thrombocythemia (ET), or myelofibrosis (MF). Strikingly, individuals with a *JAK2*^{V617F} mutation have a 6-fold increase in thrombosis risk [2,3]. Collectively, these data suggest that dysfunctional JAK-STAT signaling in MPNs contributes to increased vascular activation and thrombosis risk.

Vascular endothelial cell activation is a hallmark of various pathologies, including MPNs, sickle cell disease [4], and COVID-19 [5–12]. Markers of vascular activation include increased secretion of von Willebrand factor (VWF) and P-selectin from preformed granules within Weibel-Palade bodies, increased procoagulant tissue factor expression, and expression of proadhesive markers, such as vascular cell activation marker (VCAM-1) and intracellular adhesion molecule 1 (ICAM-1) [13]. Physiologically, vascular endothelial activation serves to recruit leukocytes and platelets and facilitate hemostasis, immune regulation, and angiogenesis. Interestingly, both *in vitro* and *in vivo* studies suggest that the endothelium in *JAK2*^{V617F} MPNs contributes to the thrombotic risk through increased expression of VWF and P-selectin [14,15]. Furthermore, downstream of the *JAK2*$^{V617F+}$ mutation, STAT3 activation is known to increase endothelial cell (EC) expression of cell adhesion molecules [16,17]. Collectively, these data suggest that JAK-STAT signaling in ECs increases thrombotic risk by driving procoagulant and proadhesive protein expressions. Moreover, these data suggest that the inhibition of JAK-STAT signaling may reduce vascular activation.

Ruxolitinib, a JAK1/JAK2 kinase inhibitor, was the first approved agent for use in patients with *JAK2*^{V61F} PV or MF who are refractory to, or intolerant of, hydroxyurea [18]. Fedratinib, a more selective JAK2 inhibitor, is currently the only other JAK inhibitor

approved for the front-line use in MF [19]. In PV, ruxolitinib alleviates constitutional symptoms, lowers hematocrit, and reduces spleen size and cell number [20,21]. However, there is only limited clinical data on the reduction of thrombotic events [21,22]. Furthermore, there is postmarketing analysis that ruxolitinib may increase the pulmonary embolism rates [23]. Fedratinib, approved in 2019 but in use since 2008, has no thrombotic event data reported. Beyond ruxolitinib and fedratinib, there are other JAK inhibitors either approved or undergoing phase 1–3 trials for use for various pathologic conditions, including MPNs, graft-vs-host disease, pancreatic cancer, rheumatoid arthritis, and COVID-19 [24–27]. However, many of these JAK-STAT inhibitors contain black-box warnings regarding increased thrombosis risk [23,28–30]. Therefore, evaluation to determine whether JAK-STAT inhibitors contribute to increased thrombotic risk is warranted.

Herein, we sought to determine whether JAK-STAT inhibitors reduce prothrombotic and inflammatory signaling in endothelial cells. By using TNF-α stimulation, we found that treatment with either ruxolitinib or fedratinib reduced phospho-STAT1 and 3 and that fedratinib attenuated nuclear c-Jun activation. In functional assays, ruxolitinib or fedratinib reduced secretion of P-selectin and VWF and soluble interleukin 6 (sIL-6) and tissue factor from endothelial cells. In addition, ruxolitinib or fedratinib reduced expression and activity of tissue factor and urokinase plasminogen activator. Finally, in endothelialized microfluidics, we demonstrated that treatment of endothelium with JAK-STAT inhibitors prevented leukocyte rolling in whole blood from healthy individuals and individuals with the prothrombotic *JAK2*^{V617F} mutation. Altogether, we demonstrate that JAK-STAT inhibitors, alone or in the presence of inflammatory cytokines, do not increase prothrombotic VWF and P-selectin or tissue factor and decrease proadhesive leukocyte interactions.

2 | MATERIALS AND METHODS

2.1 | Chemicals and reagents

Ruxolitinib (CAS 941678–49-5, Cat#11609) and fedratinib (TG101348) were purchased from Cayman Chemical, dissolved in DMSO, and stored as 5 μl stock aliquots: 20 mM ruxolitinib at −20 °C and 10 mM fedratinib at −80 °C. Recombinant human TNF-α was obtained from R&D Systems (#210-TA). Nuclear extracts were prepared by using the kit from Cayman Chemical (#10009277) following the manufacturer's guidelines. Protein was quantified by using the Pierce BCA Protein Assay Kit (ThermoScientific Cat#23225). Human factor X (#HCX-0050) and human factor VIIa (HCVIIA-0031) were purchased from Haematologic Technologies. Chromogenic substrate for the determination of factor Xa activity (Chromogenix S-2765, Diapharma) was reconstituted per manufacturer's instructions and stored at 4 °C. The urokinase type plasminogen activator human chromogenic activity assay kit was purchased from Abcam (Cat#ab8915) and used following the manufacturer's protocol. HEPES buffered saline [HBS] (20 mM HEPES, pH 7.4, 150 mM NaCl) was used for tissue factor assay with the addition of 3% w/v bovine serum albumin (Fraction V; Fischer). CaCl2 (10 mM, final concentration) was added. For quenching the reactions, EDTA (10 mM final concentration) was added.

2.2 | Antibodies

The following antibodies were used for immunoblots: P-STAT1 Tyr701) (58D6) Rabbit mAb Cat#9167); STAT1 (D4Y6Z) Rabbit mAb #1499; P-Stat3 (Y705) (D3A7) Rabbit mAb #9145, STAT3 (79D7) Rabbit mAb#4904, P-cJun63 (Ser63)(54B3) Rabbit mAb #2361, and c-Jun (60A8) Rabbit mAb#9165; P-NF-kB p65 (Ser536) (93H1) Rabbit mAb #3033; NF-kB (D14E12) XP Rabbit mAb #8242; GAPDH (D4C6R) Mouse mAb #97166, P-p44/42 MAPK (T202Y204) (20G11) (P-Erk1/2) Rabbit mAb#4376; p44/42 MAPK (Erk1/2) Rabbit mAb #9102; P-Akt (Ser473) (D9E) XP Rabbit mAb #4060; Akt (pan)(C67E7) Rabbit mAb #4691; and P-p38MAPK(Thr180/Tyr182) (D3F9)XP Rabbit mAb #4511, all from Cell Signaling Technology.

The following antibodies were used for immunofluorsence: P-selectin (R&D Systems #AF737), VWF (vWF, Cedarlane #CL20176A-R), and VE-cadherin (R&D Systems #AF1002).

2.3 | Endothelial cell culture

Primary human umbilical vein endothelial cells (HUVEC) were isolated as previously described [31]. For static cultures, cells were grown until 95% confluent and then changed to 0.1%–1.0% FBS media. All cells were between passages 2 and 5 for experiments.

2.4 | Human blood samples

Blood samples were obtained in sodium citrate vacutainers from healthy adult volunteers and MPN patients after obtaining informed consent and according to the protocols approved by the University of Minnesota's Institutional Review Board in accordance with the Declaration of Helsinki.

2.5 | Confocal microscopy

HUVEC grown in 0.1% FBS media were incubated with ruxolitinib (0.4 μM) or fedratinib (1 μM) JDB for 30 minutes followed by the addition of 10 ng/mL TNF-α (R&D Systems) JDB. After 4 hours, cells were fixed with 4% paraformaldehyde and stained with primary antibodies. Primary antibodies were identified with the appropriate fluorescent-labeled secondary antibodies (Jackson Immunoresearch). Nuclei were counterstained with 4',6-diamidino-2-phenylindole (DAPI; Invitrogen). Cells were visualized, and images acquired by using a FluoView FV1000 BX2 upright confocal microscope (Olympus) with UPlanSApo 20X/0.80 and UPlanApo N 60X/1.42 objectives with zoom (Z) 2 as indicated. Images were processed with FluoView (Olympus) and Adobe Photoshop software.

2.6 | Immunoblots

HUVEC grown in 1% FBS media were incubated with ruxolitinib (0.4 μM) or fedratinib (1 μM) JDB for 30 minutes followed by the addition of 10 ng/mL TNF-α (R&D Systems) JDB. After 4 hours, the total protein extract or nuclear extract was collected. Protein concentration values were obtained with the BCA kit (Pierce). Lysates were run on 10% Mini-PROTEAN TGX Precast Protein Gels, 12-well, 20 μl (Cat#4561035), with 6–20 mg protein/lane, transferred to polyvinylidene difluoride (PVDF) membrane and stained for total protein

by using fluorescent AzureRed Protein Stain (Azure Biosystems, Cat#AC2124). After blocking with Odyssey blocking buffer (Li-Cor), immunoblots of protein or nuclear extract subfractions were probed with primary antibodies to P-NF-kB p65, NF-kBp65, P-STAT1, STAT1, P-STAT3, STAT 3, P-cJun63, and c-Jun and loading control mouse GAPDH (Cell Signaling Technology), diluted 1:1000. Primary antibodies were detected with appropriate secondary antibodies from AzureSpectra conjugated to fluorescent or near-infrared ranges and visualized by using an Azure c600 imager (Azure, Biosciences). Experiments were performed at least 3 times. Images were quantified by using FIJI software (NIH).

2.7 | Conditioned media assessment

HUVEC were cultured in 24-well plates with incubation in 1% HUVEC media with ruxolitinib (0.4 μM) or fedratinib (1 μM) JDB for 30 minutes followed by the addition of 10 ng/mL TNF-α (R&D Systems) for 4 hours. Conditioned media were collected and spun at 1500 ×*g* at 4 °C for 15 minutes and stored at −20 °C. P-selectin, tissue factor, IL-6, and sVCAM-1 were measured by using the multiplex cytokine array (Thrombosis mix and match panel; BioLegend). VWF antigen was measured by using human VWF antigen ELISA kit (Molecular Innovations).

2.8 | RNA analysis

RNA was extracted by using the RNeasy kit (Qiagen), followed by cDNA generation according to the manufacturer's protocol (Bio-Rad). Custom Endothelial Coagulation RNA array (Bio-Rad PrimePCR) was used to assess gene expression, with each reaction containing 30 ng of cDNA, lyophilized primers, and SSoAdvanced SYBR Green QPCR master mix. The PCR conditions included activating the DNA polymerase at 95 °C for 10 minutes, followed by 40 cycles of 3 step PCR (95 °C for 10 seconds, 60 °C for 30 seconds). Melt curves for each primer set were run and verified.

Cycle threshold (*Ct*) values from samples of each gene and the internal control (RPLP0) were obtained, and the relative quantification for each gene was calculated by using the $\Delta\Delta Ct$ method [20].

2.9 | Coagulation assays

For tissue factor (TF) generation, treated HUVECs were cultured for 30 minutes in the presence of anti-TF antibody (BD Biosciences) or isotype IgG control (BD Biosciences) along with recombinant factor VIIa (100 pM, final concentration), factor X (135 nM, final concentration Enzyme Research Laboratories), and 5 mM calcium in HBS-BSA buffer. After 30 minutes, the sample was quenched with EDTA, and chromogenic Xa generation was conducted by using 0.5 mM Chromagenix FXa and reading absorbance at 450 nm every 30 seconds on a plate reader (Molecular Technologies).

For uPA activity, HUVECs grown in 24-well plates were incubated in 1% FBS media with ruxolitinib (0.4 μM) or fedratinib (1 μM) JDB for 30 minutes followed by the addition of 10 ng/mL TNF-α (R&D Systems) JDB for 4 hours. Conditioned media were collected and spun at 1500 ×*g* at 4 °C for 15 minutes and stored at −80 °C. Conditioned media were assessed for uPA activity over 4 hours at 37 °C following the manufacturer's direction (Abcam).

2.10 | Microfluidics devices

2.10.1 | Fabrication—A single-layer microfluidic device was fabricated as a platform to study leukocyte and platelet velocity. The device design included one long resistor with 8 straight sections, with one inlet port and one outlet port. The device consisted of a polymethyl siloxane (PDMS) microchannel layer (405 144 μm [Length] × 1000 μm [Width] × 50 μm [Height]) bonded to a glass substrate. The PDMS layer of the device was fabricated by using a soft photolithography mask designed using AutoCAD (Autodesk). A master mold was created by coating a negative photoresist onto a silicon substrate followed by UV light exposure and removal of excess material. The master mold was used to generate the PDMS-based channel layer. The PDMS layer and glass substrate were coated in O2 plasma for 2 minutes and then bonded together followed by the evaporation of excess water molecules through incubation for 1 hour on a hot plate set to 110 °C.

2.10.2 | HUVEC culture in devices—Microfluidic devices were coated with 2% gelatin solution for 3 minutes at room temperature. ECs (passages 2–5) were trypsinized and resuspended in EGM-2 cell culture medium supplemented with a EGM-2 SingleQuots growth kit (Lonza) at a density of 1.0×10^6 cells/μL. ECs were then pipetted into the inlet port of the device until all channels were evenly covered. Devices were incubated at 37 °C, 5% CO2 for 30 minutes to allow for cell adherence. In addition, 3-mL syringes (BD) were filled with EGM-2 and connected to 0.020 inch ID plastic tubing (Tygon). The plastic tubing was connected to the inlet port of the device, and the syringe was secured in a syringe pump (kd Scientific). The syringe pump was set to a flow rate of 50 μL/hour for 24 hours, and devices were place at 37 °C, 5% CO2. After 24 hours, 3-mL syringes were switched out for 60-mL syringes, and the flow rate was changed to 2 mL/h for the next 48 hours. After 48 hours, the devices were ready for subsequent treatment.

2.10.3 | Treatment of devices—Before flowing blood through, endothelialized devices were treated by adding 10 ng/mL TNFα, 0.4 μM ruxolitinib, 1 μM fedratinib, JDB or combination treatment (Rux+TNF or Fed+TNF) into EGM-2 media followed by incubation for 4 hours at 37 °C, 5% CO2 with a flow rate of 2 mL/h (15 dyne/cm^2). Each device corresponded to one treatment condition.

2.10.4 | Fluorescence imaging—On the day of the experiment, blood samples were obtained and labeled with calcein live stain (BioLegend) to tag leukocytes and platelets, 15 minutes before running the sample. Labeling of cells was confirmed by using blood smear before loading the sample into the microfluidic device. The labeled sample was loaded into a 1 mL syringe (BD) and set into a syringe pump running at a flow rate of 150 μL/h (1 dynes/cm^2). Endothelialized microfluidic devices were disconnected from the syringe pumps containing EGM-2 and reconnected to the 1 mL syringe containing patient blood on a microscope stage. As blood flowed through the devices, 10-second videos were captured of at least 2 nonoverlapping regions of interest (ROI)s along the 8 long, straight sections of the microchannels by using a fluorescent microscope (Zeiss) at 10× magnification. Camera speed was set to 6.4 frames per second, with an average of 64 frames per video. Video was recorded for 15 minutes per device, resulting in 12–20 videos captured per device.

2.10.5 | Image analysis—Images were processed by using FIJI (National Institutes of Health). A FIJI plugin, TrackMate [32], was used to quantify the velocity of cells passing through the ROIs described above. This camera speed excludes single platelet behavior, and events were thresholded to include tracks with between 50 and 200 spots. The mean velocity of each "track" corresponding to one cell was recorded for all of the tracks in each video captured. For each condition, the average velocity was calculated from around 6 of the total number of videos captured. The SD was calculated for each treatment condition.

2.10.6 | Statistics—Descriptive statistics are presented as mean ± SE. Normality assessments were conducted for all comparisons. Analysis for each experiment is included in the legends, with multiple comparisons analyzed by using ANOVA with the Holm–Sidak method or Kruskal–Wallis with the Dunn's test for multiple comparisons using GraphPad Prism (v 9). Statistical significance was defined by a p value less than .05.

3 | RESULTS

3.1 | Ruxolitinib and fedratinib reduce TNF-α mediated endothelial cell kinase signaling

To identify the concentration of ruxolitinib or fedratinib sufficient to inhibit JAK-STAT signaling, we stimulated endothelial cells with TNF-α to activate STATs in the presence or absence of ruxolitinib or fedratinib and then quantified STAT1 and STAT3 phosphorylation by western blots (Figure 1A). At 4 hours, compared with TNF-α alone, treatment with either 0.4 μM ruxolitinib or 1 μM fedratinib significantly reduced STAT1 (Figure 1B) and STAT3 signaling (Figure 1C) at similar levels. At 24 hours, compared with untreated cells, there was some persistent elevation of phospho-STAT1, which ruxolitinib and fedratinib reduced. For STAT3, compared with untreated cells, TNF-α alone continued to increase phospho-STAT3, with a significant reduction by ruxolitinib and mild reduction by fedratinib (Supplementary Figure S1). Next, to assess critical proinflammatory signaling pathways after 4-hour stimulation with TNF-α, we probed for effects on proinflammatory NF-κB phospho-p65, c-Jun (Figure 1A), phospho-ERK, phospho-Akt, and phospho-p38 MAPK (Supplementary Figure S2). Compared with untreated endothelial cells, neither ruxolitinib nor fedratinib alone increased c-Jun (Figure 1D) or NF-κB phospho-p65 (Figure 1E). By contrast, TNF-α significantly increased both c-Jun (Figure 1D) and NF-κB phospho-p65 (Figure 1E). When added to TNF-α, ruxolitnib had minimal to no effect on reducing c-Jun (Figure 1D) or NF-κB phospho-p65 (Figure 1E). Interestingly, fedratinib, a more selective JAK2 inhibitor, demonstrated a modest, nonsignificant reduction in c-Jun and NF-κB phospho-p65 nuclear localization. There was no effect on phospho-ERK, phospho-p38MAPK, or phospho-Akt (Supplementary Figure S2). Combined, these data demonstrate that ruxolitinib and fedratinib block proinflammatory signaling through STAT1 and STAT3 and that fedratinib may attenuate c-Jun and NF-κB phospho-p65 nuclear localization.

3.2 | Ruxolitinib and fedratinib reduce TNF-α mediated endothelial P-selectin and VWF surface expression and reduce of proinflammatory and thrombotic marker expression

Endothelial activation leads to release of preformed Weibel-Palade bodies containing prothrombotic VWF and proadhesive P-selectin. To evaluate whether treatment with JAK-STAT inhibitors reduces surface expression of VWF and P-selectin as a surrogate for

Weibel-Palade body release, we performed confocal imaging of HUVEC in the presence of ruxolitinib or fedratinib ± TNF-α to assess cell-associated P-selectin and VWF. Compared with untreated cells or cells treated with ruxolitnib or fedratinib alone, cells treated with TNF-α exhibited an increase in P-selectin release and VWF surface expression (Figure 2A, B). Compared with TNF-α alone, cells treated with TNF-α + ruxolitinib or fedratinib displayed reduced surface expression of P-selectin and VWF (Figure 2A, B). To verify these findings, we performed P-selectin and VWF ELISAs on conditioned medium from HUVEC treated with ruxolitinib and fedratinib ± TNF-α. Compared with untreated HUVEC, neither ruxolitnib nor fedratinib alone increased P-selectin or VWF release. Addition of TNF-α significantly increased both P-selectin and VWF levels (Figure 2C, D). Compared with TNF-α alone, addition ofeither ruxolitnib or fedratinib with TNF-α reduced P-selectin secretion (Figure 2C). Similarly, compared with TNF-α alone, addition of ruxolitinib to TNF-α reduced VWF secretion (Figure 2D), with fedratinib cotreatment exhibiting a modest VWF reduction. Collectively, these data demonstrate that both ruxolitnib and fedratinib reduce surface expression of P-selectin and VWF from TNF-α stimulated endothelial cells.

Besides P-selectin and VWF, endothelial cell activation is also known to stimulate increased expression of proinflammatory and thrombotic mediators, such as interleukin 6 (IL-6) and TF. Therefore, we next assessed the release of these proinflammatory and thrombotic markers. First, by using cytokine arrays, we performed the analysis of conditioned medium from endothelial cells for proinflammatory IL-6 and TF. Compared with untreated cells, treatment with either ruxolitnib or fedratinib alone did not increase conditioned medium levels of soluble IL-6 (sIL-6) or TF (Figure 2E, F). Consistent with endothelial activation, TNF-α treatment significantly increased sIL-6 and TF levels. Compared with TNF-α alone, ruxolitinib cotreatment did not reduce sIL-6 release; however, fedratinib cotreatment exhibited a significant reduction in sIL-6 levels (Figure 2E). Compared with TNF-α alone, TNF-α cotreatment with either ruxolitinib or fedratinib resulted in significant reduction in TF release (Figure 2F). Overall, these data demonstrate that both ruxolitinib and fedratinib reduce proinflammatory and prothrombotic TNF-α-mediated endothelial activation.

3.3 | Ruxolitinib and fedratinib reduce TNF-α mediated upregulation of tissue factor and urokinase genes

Because JAK-STAT inhibition reduced TNF-α-mediated endothelial activation with decreased soluble TF, we evaluated whether treatment with ruxolitinib or fedratinib would reduce transcription of the downstream procoagulant TF gene (Factor 3, *F3*). Compared with untreated HUVEC cells, TNF-α resulted in significant upregulation of *F3* mRNA (Figure 3A). Treatment with ruxolinitib or fedratinib alone had no effect on *F3* mRNA expression. However, in combination with TNF-α, both ruxolitinib and fedratinib significantly reduced *F3* mRNA upregulation (Figure 3A). In addition, by using microscopy, we observed that compared with TNF-α alone, surface TF expression was decreased by either ruxolitinib or fedratinib cotreatment (Supplementary Figure S3).

Urokinase, a serine protease critical in modulating fibrinolysis, expression is known to be downstream of JAK-STAT signaling [33]. Therefore, we also assessed expression of urokinase mRNA (*PLAU*). Compared with untreated endothelial cells, TNF-α treatment

significantly upregulated *PLAU* mRNA (Figure 3B). The addition of either ruxolitinib or fedratinib with TNF-α significantly decreased *PLAU* mRNA (Figure 3B). Of note, there was no significant downregulation of proadhesive *VCAM-1* mRNA, which uses PKC signaling and NF-κB, for transcription (Supplementary Figure S4). In addition, consistent with the potential decrease in release of preformed Weibel-Palade bodies, neither ruxolitinib nor fedratinib decreased the VWF mRNA levels (Supplementary Figure S4). Collectively, these data suggest that the inhibition of endothelial JAK-STAT signaling reduces the transcription of procoagulopathic TF and fibrinolytic urokinase.

3.4 | Ruxolitinib and fedratinib reduces TNF-α mediated tissue factor and urokinase activity

As we observed a decrease in TF and urokinase gene expression, we next sought to determine whether JAK-STAT inhibition decreases EC TF and urokinase activation. Therefore, we performed surface TF activity and urokinase activity assays. Treatment with vehicle (DMSO), ruxolitinib, or fedratinib did not increase surface TF activity (Figure 3C). Compared with untreated endothelial cells, TNF-α treated endothelial cells exhibited significantly higher TF activity (Figure 3C). Addition of ruxolitinib or fedratinib to TNF-α suppressed endothelial TF activity (Figure 3C). Notably, the assessment of other JAK-STAT inhibitors, such as solcitinib (JAK2), momelotinib (JAK1/2), and tofacitinib (JAK3), also demonstrate a similar pattern with reduced TNF-α stimulated TF activity (Supplementary Figure S5). Collectively, these data suggest that JAK-STAT inhibitors reduce EC TF protein and activity.

Urokinase is secreted by endothelial cells to catalyze the activation of plasminogen to plasmin; therefore, we measured the urokinase activity in conditioned medium from endothelial cells treated with or without JAK-STAT inhibitors. Compared with untreated cells, neither ruxolitinib nor fedratinib alone increased urokinase activity (Figure 3D). Compared with untreated endothelial cells, TNF-α treated endothelial cells exhibited significantly higher urokinase activity. Addition of either ruxolitnib or fedratinib to TNF-α suppressed urokinase activity (Figure 3D). The decrease in urokinase activity was not owing to the increased PAI-1 levels (Supplementary Figure S6). Collectively, these data suggest that JAK-STAT inhibitors prevent inflammation-mediated increase in TF and urokinase activity in endothelial cells.

3.5 | Ruxolitinib and fedratinib reduce TNF-α mediated leukocyte–endothelial interactions

Leukocyte and platelet adhesion and rolling on the cell surface requires expression of P-selectin [34,35]. Because we observed decreased TNF-α-mediated release of P-selectin and VWF after ruxolinitib and fedratinib cotreatment, we sought to explore whether the treatment of activated endothelial cells with either ruxolitinib or fedratinib prevents leukocyte rolling. We established an endotheliazed microfluidics model workflow (Figure 4A). These endothelialized devices were first treated with ruxolinib or fedratinib alone or in combination with TNF-α. We then evaluated the rolling of calcein-labeled whole blood from healthy controls and individuals with *JAK2*^{V617F} mutation (Figure 4B, C; Table 1, Supplementary Videos S1–12). Compared with untreated endothelial cells, endothelium treated with either ruxolinib or fedratinib alone did not change the healthy control whole

blood cell velocity. Consistent with endothelial activation, TNF-α treatment significantly reduced healthy control whole blood cell velocity (Figure 4B). Compared with TNF-α alone, TNF-α cotreatment of endothelium with ruxolinitb or fedratinib increased healthy control cell velocities. Collectively, these data suggest that ruxolitinib and fedratinib reduce proadhesive interactions between activated endothelium and leukocytes.

At present, ruxlitinib and fedratinib are clinically used to treat individuals with MPN, namely PV (ruxolitinib) and MF (ruxolitinib and fedratinib). In transfection models, Guy et al. demonstrated that compared with endothelial cells expressing *JAK2*^{WT}, *JAK2*^{V617F}-expressing endothelial cells have increased P-selectin and VWF [15]. However, in *in vitro* models, leukocyte rolling was only increased when *JAK2*^{V617F} mice were treated with TNF-α. In addition, although *JAK2*^{V617F} endothelial cells have been detected in MPN patients, the location and distribution of mutation within the vasculature is unknown. Recent work suggests that even in individuals who have experienced thrombosis, endothelial *JAK2*^{V617F} expression may not be consistently present [36]. Therefore, to isolate the effects of ruxolitinib and fedratinib on interactions between *JAK2*^{V617F} leukocytes and activated endothelium, we collected whole blood from individuals diagnosed with MPN (PV, ET, or MF) who have a *JAK2*^{V617F} mutation followed by assessment in our TNF-α endothelialized models. Consistent with myeloproliferative diagnosis, compared with healthy control donors, individuals with *JAK2*^{V617F} mutation had significantly higher hematocrit and platelet counts (Table 1).

When comparing cell velocity between control donors and *JAK2*^{V617F} individuals, there were no significant differences in cell velocity. Compared with untreated endothelial cells, endothelium treated with either ruxolinib or fedratinib did not change *JAK2*^{V617F} blood cell velocity. Treatment of endothelium with TNF-α significantly reduced *JAK2*^{V617F} blood cell velocity (Figure 4C). Compared with TNF-α alone, addition of ruxolitinib or fedratinib to TNF-α-treated endothelium increased *JAK2*^{V617F} cell velocity (Figure 4C).

Collectively, these data suggest that in the vasculature, JAK-STAT inhibitors mitigate the proadhesive phenotype and reduce rolling of proadhesive *JAK2*^{V617F} leukocytes.

4 | DISCUSSION

JAK-STAT inhibitors, originally designed to treat *JAK2*^{V617F}-mutated MPN, are increasingly being used to treat other proinflammatory conditions, such as graft-vs-host disease [27], pancreatic cancer [37], rheumatoid arthritis [30,38,39], and COVID-19 [24]. However, post-marketing and clinical data suggest that many JAK-STAT inhibtors may increase thrombosis risk [23,29,30,40]. Therefore, we sought to define whether JAK-STAT inhibitors reduce vascular inflammation. Using TNF-α stimulation to activate endothelial cells, we demonstrate that treatment with ruxolitinib or fedratinib reduces proinflammatory signaling, specifically, reducing proadhesive P-selectin and VWF and proinflammatory IL-6 cytokine secretion.

Likewise, JAK-STAT inhibition reduced endothelial expression and activity of procoagulant TF and urokinase plasminogen activator. Finally, by using endothelialized microfluidics,

we found that treatment of the endothelium with JAK-STAT inhibitors prevented TNF-α mediated leukocyte rolling in both healthy controls and *JAK2*^{V617F} individuals.

JAK-STAT inhibitors were initially designed to target JAK2 to reduce the effects of the *JAK2*^{V617F} mutation, which leads to constitutive JAK2 activation [24]. Because thrombosis is a major driver of MPN-related mortality, the possibility that ruxolitinib and other JAK-STAT inhibitors increase vascular dysfunction has been an urgent concern. Thus far, several meta-analyses of MPN studies have yet to establish whether ruxolitinib prevents thrombosis [21,22]. Furthermore, because fedratinib is used only in myelofibrosis patients, for whom thrombosis is not the most urgent concern, there are minimal data regarding fedratinib and thrombosis.

Besides JAK2, the JAK-signaling family contains the following 3 other proteins with a similar ATP-binding pocket: JAK1, JAK3, and TYK2. Many approved or investigational JAK-STAT inhibitors exhibit variable avidity and affinity for other JAK isoforms or other kinases; for example, ruxolitinib exhibits JAK1 and JAK2 inhibition, whereas fedratinib inhibits JAK2 and Flt3 and RET. This is notable, as in the setting of MPN, which is a prothrombotic condition, the possibility that JAK inhibitors may increase thrombotic risk is not trivial, given that several other FDA-approved JAK-STAT inhibtors carry black-box warnings related to prothrombotic potential. For example, tofacitinib, an oral JAK 3 inhibitor, is approved for proinflammatory conditions, such as rheumatoid arthritis. In the RA population, compared with TNF-α inhibitors, tofacitinib use was associated with increased adverse cardiovascular outcomes, including thrombosis [23,30,41]. However, several factors, including JAK isoform avidity, chronicity of inflammation, and other co-morbidities, including diabetes and hypertension, may influence the pro- and antithrombotic balance. In addition, regarding *JAK2*$^{V617F+}$ malignancies, work published by Brkic et al. demonstrates that *JAK2*$^{V617F+}$ malignancies use other signaling pathways, such as phospho-ERK, to evade/escape JAK-STAT inhibition [42]. Collectively, these data suggest that proinflammatory/thrombotic signaling pathways beyond JAK-STAT signaling may contribute to increased prothrombotic cell adhesion.

Beyond the vasculature, mechanistically, another recent *in vivo* study, using a *JAK2*^{V617F} mouse model, demonstrated that ruxolitinib had an antithrombotic effect through reduction in neutrophil extracellular traps (NETs) [43]. Likewise, a limited flow cytometry pilot study comparing prothrombotic markers in *JAK2*$^{V617F+}$ patient samples before and after starting ruxolitinib found that monocyte TF expression and monocyte number were reduced after starting ruxolitinib [40]. The reduction in TF is notable because a larger study comparing *JAK2*$^{V617F+}$ patients with thrombosis history with those without found that in subjects with thrombosis history, granulocyte tissue expression was upregulated 13-fold [44]. Similarly, compared with healthy controls, individuals with *JAK2*$^{V617F+}$ PV or ET were found to have increased neutrophil TF activity [45]. In addition, in MPN patients with a history of thrombosis, there was an observed increase in tissue factor-bearing platelet microvesicles [46,47].

In our study, only the endothelium, not leukocytes or platelets, was treated with JAK-STAT inhibitors. Therefore, it is notable that we also observed reduced endothelial TF

expression and activity with JAK-STAT inhibition. Furthermore, the effect on surface TF activity was noted not only in endothelial cells treated with ruxolitinib and fedratinib but also in the endothelial cells treated with other JAK-STAT inhibitors, including tofacitinib (Supplementary Figure S5), which is consistent with previously published work using a broader tissue-specific platform [48]. Collectively, these data suggest that within the vasculature, JAK-STAT inhibitors do not increase endothelial TF activation.

We chose to evaluate our findings by using endothelialized microfluidics because there are >10 different *JAK2*$^{V617F+}$ MPN mouse models reported in the literature [49–51]; each *JAK2*$^{V617F+}$ MPN model exhibits varying PV/ET or MF phenotypes depending on allelic expression and location of transgene expression [50–52]. For example, mice with inducible EC *JAK2*$^{V617F+}$ transgenic expression also have an ET-like phenotype, but exhibit an acquired VWF-like bleeding diathesis [6]. Of note, Wolach et al. used bone marrow chimera mice lacking endothelial *JAK2*^{V617F} expression to demonstrate thrombosis. Likewise, in a tamoxifen-inducible cre (*Pdgfb-iCreERT2;JAK2*$^{V617F/WT}$) endothelial restricted model, TNF-α was required to induce pulmonary thrombi [15]. To address the limitations in MPN mouse models, we sought to create a model under flow by which endothelial activation is secondary to drug exposure because most murine thrombosis models use surgical techniques that create direct endothelial damage through either surgical ligation or electric injury [53,54]. Therefore, adoption of an endothelialized microfluidics model permits for more stringent experimental parameter control. By using our model, we found that treatment with JAK-STAT inhibitors alone does not increase adhesion of either healthy or *JAK2*$^{V617F+}$ leukocytes. Furthermore, in the presence of proinflammatory stimuli, such as TNF-α, JAK-STAT inhibition reduced leukocyte rolling. Collectively, our data, by using normal and MPN whole blood, suggest that JAK-STAT inhibitors do not increase endothelial proadhesive interactions.

In PV patients with previous splanchnic thrombosis, at least 3 studies demonstrate endothelial *JAK2*^{V617F} expression [55–57]. Several other studies have also derived *JAK2*^{V617F} endothelial cells from stem cells [14] or used lentiviral constructs to transduce *JAK2*^{V617F} expression *in vitro* [15]. Likewise, there are several reports of isolating endothelial colony forming cells from *JAK2*^{V617F} individuals [58–60]. Collectively, these studies demonstrate that *JAK2*^{V617F} endothelial cells likely contribute to the prothrombotic mileu in MPN. However, it is notable that a recent publication found that endothelial colony forming cells from *JAK2*^{V617F} individuals may not uniformly exhibit *JAK2*^{V617F} expression [36]. This suggests that transgenic *JAK2*^{V617F} mice with 100% endothelial expression of *JAK2*^{V617F} may not be physiologic.

In addition, we sought to determine whether JAK-STAT inhibitors themselves increased prothrombotic/adhesive behavior. Therefore, we chose to evaluate *JAK2*^{V617F} leukocyte–endothelial interactions by using TNF-α endothelial cells in our fluidics models instead of *JAK2*^{V617F} endothelial cells. Overall, there have been more than 79 different cytokines found to have aberrant levels in *JAK2*^{V617F} MPNs; therefore, our work does not capture the effects of other prothrombotic stimuli, such as IL-1β or interferon. However, because it has previously been used in previous experiments with *JAK2*^{V617F} endothelial cells, we selected TNF-α to stimulate our endothelial cells [15]. Furthermore, we chose our concentration and

time points based on similar *in vitro* studies and preliminary studies evaluating signaling (Supplementary Figure S1) [15]. Overall, our model agrees with both *in vitro* and *in vivo* studies that note significant differences in leukocyte rolling and adhesion on $JAK2^{V617F+}$ endothelial cells only *after* TNF-α stimulation [14,15]. Moving forward, both *in vitro* and *in vivo* studies evaluating the role of other stimulants, such as IL-1β, may be useful in $JAK2^{V617F+}$ MPN. Overall, combined with the literature, our model and data suggest that increased endothelial expression of procoagulant and proadhesive proteins, such as VWF or P-selectin, may contribute to increased $JAK2^{V617F}$ procoagulant behavior and that JAK-STAT inhibition reduces endothelial expression of these critical proteins [61,62].

Because the use of JAK-STAT inhibitors in not confined to just MPN patients, our microfluidics studies evaluated blood from both healthy controls and MPN patients with the $JAK2^{V617F}$ mutation. Consistent with MPN diagnosis, individuals with the $JAK2^{V617F}$ mutation had higher hematocrit and platelet counts than healthy controls. However, because of the camera speed limitations, our studies do not fully capture platelet-dependent adhesion events. We anticipate future studies by using platelet-specific markers to address this important translational question. Furthermore, our current devices require a fixed pressure, which limits the ability to ascertain the contribution of hematocrit or viscosity on the proadhesive and thrombotic milieu. We anticipate future work to incorporate variable pressure into our microfluidics model. Finally, our studies excluded MPN patients on systemic anticoagulation, which is a population at the highest risk for recurrent thromboembolic events. However, despite these limitations, our studies provide valuable context regarding endothelial–leukocyte interactions after JAK-STAT inhibition at the level of the vasculature; this is important because we provide data suggesting that JAK-STAT inhibitors alone do not increase or contribute to vascular activation.

5 | CONCLUSION

JAK-STAT inhibitors, originally designed to treat individuals with $JAK2^{V617F}$ mutation, are now in consideration for us in various proinflammatory conditions. We demonstrate that inhibition of JAK-STAT signaling pathways reduces TNF-α-mediated activation of endothelial cells by reducing proinflammatory STAT signaling. We found that JAK-STAT inhibition reduced secretion of proadhesive P-selectin and VWF and IL-6.

Furthermore, JAK-STAT inhibition reduced endothelial TF activity. Importantly, by using endothelialized microfluidics perfused with whole blood from healthy controls or MPN patients with $JAK2^{V617F}$ mutations, we found that ruxolitinib or fedratinib reduced proadhesive cell interactions. Collectively, this work demonstrates that the JAK-STAT pathway contributes to vascular activation and that JAK-STAT inhibitors reduce critical proadhesive and prothrombotic markers.

Supplementary Material

Refer to Web version on PubMed Central for supplementary material.

ACKNOWLEDGMENTS

The authors would like to thank Michael Franklin, MS for editorial assistance in manuscript preparation. The authors would like to thank Muse Jama, Amy Eisenberg, Diondra Howard, Ghislaine Feussom, and Rebecca Cote for assistance with acquiring whole blood samples from volunteers. The authors also thank Drs. Nigel Key, John Belcher, and Robert Hebbel for helpful comments and insights.

FUNDING INFORMATION

J.D.B. is supported in part by NHLBI K08HL159289, Institutional Research Grant #129819-IRG-16-189-58-IRG-114 from the American Cancer Society, Masonic Cancer Research Translational Initiative Research Grant, an American Heart Association Career Development Award and American Society of Hematology Restart Award. A.D.S. is supported by T32-HL139341. D.R. received funding from University of Minnesota Life Sciences Undergraduate Research Program (LSSURP) 5R25HL088728-14. Academic Investment in Research Program Grant supports G.M.V. D.K.W. is supported by R01HL140589 and HL132906. Portions of this work were conducted in the Minnesota Nano Center, which is supported by the National Science Foundation through the National Nanotechnology Coordinated Infrastructure (NNCI) under Award Number ECCS-2025124. Other portions were supported by the resources and staff at the University of Minnesota University Imaging Centers (UIC), SCR_020997. Database and Biostatistic support was provided by Clinical and Translational Science Institute grant support (UL1TR002494 from the National Institutes of Health's National Center for Advancing Translational Sciences).

DECLARATION OF COMPETING INTERESTS

J.D.B. receives funds from Bayer independent from work herein. G.M.V. receives research funding from CSL Behring and Mitobridge (Astellas). C.B. has received reagents from CTI BioPharma for the conduct of clinical trial NCT 02891603 and a pending patent, WO2017058950A1, for methods of treating transplant rejection. B.C.B. holds patents related to CD4+ T cell pSTAT3 as a marker and therapeutic target of acute GVHD (WO2015120436A2); for the use of JAK inhibitors for rejection and GVHD prevention (WO2017058950A1); and for the use of CD83-targeted chimeric antigen receptor T cells in GVHD prevention, immune tolerance, autoimmunity, and acute myeloid leukemia therapy (WO2019165156). At this time, neither B.C.B. nor the University of Minnesota has received payment related to claims described in the patent. B.C.B. has received honoraria for participating in advisory board discussions for Incyte Corp and CTI BioPharma within the past 5 years.

REFERENCES

[1]. Perner F, Perner C, Ernst T, Heidel FH. Roles of JAK2 in aging, inflammation, hematopoiesis and malignant transformation. Cells. 2019;8. [PubMed: 31861404]

[2]. Cordua S, Kjaer L, Skov V, Pallisgaard N, Hasselbalch HC, Ellervik C. Prevalence and phenotypes of JAK2 V617F and calreticulin mutations in a Danish general population. Blood. 2019;134:469–79. [PubMed: 31217187]

[3]. Mehta J, Wang H, Iqbal SU, Mesa R. Epidemiology of myeloproliferative neoplasms in the United States. Leuk Lymphoma. 2014;55:595–600. [PubMed: 23768070]

[4]. Hebbel RP, Belcher JD, Vercellotti GM. The multifaceted role of ischemia/reperfusion in sickle cell anemia. J Clin Invest. 2020;130: 1062–72. [PubMed: 32118586]

[5]. Lussana F, Rambaldi A. Inflammation and myeloproliferative neoplasms. J Autoimmun. 2017;85:58–63. [PubMed: 28669446]

[6]. Etheridge SL, Roh ME, Cosgrove ME, Sangkhae V, Fox NE, Chen J, Lopez JA, Kaushansky K, Hitchcock IS. JAK2V617F-positive endothelial cells contribute to clotting abnormalities in myeloproliferative neoplasms. Proc Natl Acad Sci U S A. 2014;111:2295–300. [PubMed: 24469804]

[7]. Dupont A, Rauch A, Staessens S, Moussa M, Rosa M, Corseaux D, Jeanpierre E, Goutay J, Caplan M, Varlet P, Lefevre G, Lassalle F, Bauters A, Faure K, Lambert M, Duhamel A, Labreuche J, Garrigue D, De Meyer SF, Staels B, et al. Vascular endothelial damage in the pathogenesis of organ injury in severe COVID-19. Arterioscler Thromb Vasc Biol. 2021;41:1760–73:Atvbaha120315595. [PubMed: 33626910]

[8]. O'Sullivan JM, Gonagle DM, Ward SE, Preston RJS, O'Donnell JS. Endothelial cells orchestrate COVID-19 coagulopathy. Lancet Haematol. 2020;7:e553–5. [PubMed: 32619412]

[9]. Goshua G, Pine AB, Meizlish ML, Chang CH, Zhang H, Bahel P, Baluha A, Bar N, Bona RD, Burns AJ, Dela Cruz CS, Dumont A, Halene S, Hwa J, Koff J, Menninger H, Neparidze N, Price C, Siner JM, Tormey C, et al. Endotheliopathy in COVID-19-associated coagulopathy: evidence from a single-centre, cross-sectional study. Lancet Haematol. 2020;7:e575–82. [PubMed: 32619411]

[10]. Kaur S, Tripathi DM, Yadav A. The enigma of endothelium in COVID-19. Front Physiol. 2020;11:989. [PubMed: 32848893]

[11]. Jung F, Krüger-Genge A, Franke RP, Hufert F, Küpper JH. COVID-19 and the endothelium. Clin Hemorheol Microcirc. 2020;75:7–11. [PubMed: 32568187]

[12]. Evans PC, Rainger GE, Mason JC, Guzik TJ, Osto E, Stamataki Z, Neil D, Hoefer IE, Fragiadaki M, Waltenberger J, Weber C, Bochaton-Piallat M, Bäck M. Endothelial dysfunction in COVID-19: a position paper of the ESC Working Group for Atherosclerosis and Vascular Biology, and the ESC Council of Basic Cardiovascular Science. Cardiovasc Res. 2020;116:2177–84. [PubMed: 32750108]

[13]. McCormack JJ, Harrison-Lavoie KJ, Cutler DF. Human endothelial cells size-select their secretory granules for exocytosis to modulate their functional output. J Thromb Haemost. 2020;18:243–54. [PubMed: 31519030]

[14]. Guadall A, Lesteven E, Letort G, Awan Toor S, Delord M, Pognant D, Brusson M, Verger E, Maslah N, Giraudier S, Larghero J, Vanneaux V, Chomienne C, El Nemer W, Cassinat B, Kiladjian JJ. Endothelial cells harbouring the JAK2V617F mutation display pro-adherent and prothrombotic features. Thromb Haemost. 2018;118:1586–99. [PubMed: 30103245]

[15]. Guy A, Gourdou-Latyszenok V, Le Lay N, Peghaire C, Kilani B, Dias JV, Duplaa C, Renault MA, Denis C, Villeval JL, Boulaftali Y, Jandrot-Perrus M, Couffinhal T, James C. Vascular endothelial cell expression of JAK2(V617F) is sufficient to promote a pro-thrombotic state due to increased P-selectin expression. Haematologica. 2019;104:70–81. [PubMed: 30171023]

[16]. Kim KJ, Kwon SH, Yun JH, Jeong HS, Kim HR, Lee EH, Ye SK, Cho CH. STAT3 activation in endothelial cells is important for tumor metastasis via increased cell adhesion molecule expression. Oncogene. 2017;36:5445–59. [PubMed: 28534515]

[17]. Wang L, Astone M, Alam SK, Zhu Z, Pei W, Frank DA, Burgess SM, Hoeppner LH. Suppressing STAT3 activity protects the endothelial barrier from VEGF-mediated vascular permeability. Dis Model Mech. 2021:14.

[18]. Vannucchi AM, Kiladjian JJ, Griesshammer M, Masszi T, Durrant S, Passamonti F, Harrison CN, Pane F, Zachee P, Mesa R, He S, Jones MM, Garrett W, Li J, Pirron U, Habr D, Verstovsek S. Ruxolitinib versus standard therapy for the treatment of polycythemia vera. N Engl J Med. 2015;372:426–35. [PubMed: 25629741]

[19]. Mullally A, Hood J, Harrison C, Mesa R. Fedratinib in myelofibrosis. Blood Adv. 2020;4:1792–800. [PubMed: 32343799]

[20]. Harrison CN, Griesshammer M, Miller C, Masszi T, Passamonti F, Zachee P, Durrant S, Pane F, Guglielmelli P, Verstovsek S, Jones MM, Hunter DS, Sun W, Li J, Khan M, Habr D, Kiladjian JJ. Comprehensive haematological control with Ruxolitinib in patients with polycythaemia vera resistant to or intolerant of hydroxycarbamide. Br J Haematol. 2018;182:279–84. [PubMed: 29984424]

[21]. Samuelson BT, Vesely SK, Chai-Adisaksopha C, Scott BL, Crowther M, Garcia D. The impact of Ruxolitinib on thrombosis in patients with polycythemia vera and myelofibrosis: a meta-analysis. Blood Coagul Fibrinolysis. 2016;27:648–52. [PubMed: 26569516]

[22]. Masciulli A, Ferrari A, Carobbio A, Ghirardi A, Barbui T. Ruxolitinib for the prevention of thrombosis in polycythemia vera: a systematic review and meta-analysis. Blood Adv. 2020;4:380–6. [PubMed: 31985808]

[23]. Verden A, Dimbil M, Kyle R, Overstreet B, Hoffman KB. Analysis of spontaneous postmarket case reports submitted to the FDA regarding thromboembolic adverse events and JAK inhibitors. Drug Saf. 2018;41:357–61. [PubMed: 29196988]

[24]. Vainchenker W, Leroy E, Gilles L, Marty C, Plo I, Constantinescu SN. JAK inhibitors for the treatment of myeloproliferative neoplasms and other disorders. F1000Research. 2018;7:82. [PubMed: 29399328]

[25]. Kalil AC, Patterson TF, Mehta AK, Tomashek KM, Wolfe CR, Ghazaryan V, Marconi VC, Ruiz-Palacios GM, Hsieh L, Kline S, Tapson V, Iovine NM, Jain MK, Sweeney DA, El Sahly HM, Branche AR, Regalado Pineda J, Lye DC, Sandkovsky U, Luetkemeyer AF, et al. Baricitinib plus remdesivir for hospitalized adults with Covid-19. N Engl J Med. 2021;384:795–807. [PubMed: 33306283]

[26]. Hoang TN, Pino M, Boddapati AK, Viox EG, Starke CE, Upadhyay AA, Gumber S, Nekorchuk M, Busman-Sahay K, Strongin Z, Harper JL, Tharp GK, Pellegrini KL, Kirejczyk S, Zandi K, Tao S, Horton TR, Beagle EN, Mahar EA, Lee MYH, et al. Baricitinib treatment resolves lower-airway macrophage inflammation and neutrophil recruitment in SARS-CoV-2-infected rhesus macaques. Cell. 2021;184:460–75.e21. [PubMed: 33278358]

[27]. Betts BC, Bastian D, Iamsawat S, Nguyen H, Heinrichs JL, Wu Y, Daenthanasanmak A, Veerapathran A, O'Mahony A, Walton K, Reff J, Horna P, Sagatys EM, Lee MC, Singer J, Chang YJ, Liu C, Pidala J, Anasetti C, Yu XZ. Targeting JAK2 reduces GVHD and xenograft rejection through regulation of T cell differentiation. Proc Natl Acad Sci U S A. 2018;115:1582–7. [PubMed: 29382747]

[28]. Kotyla PJ, Engelmann M, Giemza-Stokłosa J, Wnuk B, Islam MA. Thromboembolic adverse drug reactions in Janus kinase (JAK) inhibitors: does the inhibitor specificity play a role? Int J Mol Sci. 2021;22.

[29]. Rajasimhan S, Pamuk O, Katz JD. Safety of Janus kinase inhibitors in older patients: A focus on the thromboembolic risk. Drugs Aging. 2020;37:551–8. [PubMed: 32514874]

[30]. Ytterberg SR, Bhatt DL, Mikuls TR, Koch GG, Fleischmann R, Rivas JL, Germino R, Menon S, Sun Y, Wang C, Shapiro AB, Kanik KS, Connell CA. ORAL Surveillance Investigators. Cardiovascular and cancer risk with tofacitinib in rheumatoid arthritis. N Engl J Med. 2022;386:316–26. [PubMed: 35081280]

[31]. Beckman JD, Chen C, Nguyen J, Thayanithy V, Subramanian S, Steer CJ, Vercellotti GM. Regulation of heme oxygenase-1 protein expression by miR-377 in combination with miR-217. J Biol Chem. 2011;286:3194–202. [PubMed: 21106538]

[32]. Tinevez JY, Perry N, Schindelin J, Hoopes GM, Reynolds GD, Laplantine E, Bednarek SY, Shorte SL, Eliceiri KW. TrackMate: an open and extensible platform for single-particle tracking. Methods. 2017;115:80–90. [PubMed: 27713081]

[33]. Dumler I, Kopmann A, Weis A, Mayboroda OA, Wagner K, Gulba DC, Haller H. Urokinase activates the Jak/Stat signal transduction pathway in human vascular endothelial cells. Arterioscler Thromb Vasc Biol. 1999;19:290–7. [PubMed: 9974409]

[34]. Lawrence MB, Springer TA. Leukocytes roll on a selectin at physiologic flow rates: distinction from and prerequisite for adhesion through integrins. Cell. 1991;65:859–73. [PubMed: 1710173]

[35]. Frenette PS, Johnson RC, Hynes RO, Wagner DD. Platelets roll on stimulated endothelium in vivo: an interaction mediated by endothelial P-selectin. Proc Natl Acad Sci U S A. 1995;92:7450–4. [PubMed: 7543682]

[36]. Guy A, Danaee A, Paschalaki K, Boureau L, Rivière E, Etienne G, Mansier O, Laffan M, Sekhar M, James C. Absence of JAK2V617F mutated endothelial colony-forming cells in patients with JAK2V617F myeloproliferative neoplasms and splanchnic vein thrombosis. HematologiaSphere. 2020;4:e364.

[37]. Kasthuri RS, Hisada Y, Ilich A, Key NS, Mackman N. Effect of chemotherapy and longitudinal analysis of circulating extracellular vesicle tissue factor activity in patients with pancreatic and colorectal cancer. Res Pract Thromb Haemost. 2020;4:636–43. [PubMed: 32548563]

[38]. Hernandez G, Mills TS, Rabe JL, Chavez JS, Kuldanek S, Kirkpatrick G, Noetzli L, Jubair WK, Zanche M, Myers JR, Stevens BM, Fleenor CJ, Adane B, Dinarello CA, Ashton J, Jordan CT, Di Paola J, Hagman JR, Holers VM, Kuhn Kristine A, et al. Pro- inflammatory cytokine blockade attenuates myeloid expansion in a murine model of rheumatoid arthritis. Haematologica. 2019.

[39]. Spinelli FR, Colbert RA, Gadina M. JAK1: number one in the family; number one in inflammation? Rheumatol (Oxf Engl). 2021;60:ii3–ii10.

[40]. Keohane C, McLornan DP, Sanchez K, Connor C, Radia D, Harrison CN. The effects of JAK inhibitor therapy upon novel markers of thrombosis in myeloproliferative neoplasms. Haematologica. 2015;100:e348–50. [PubMed: 26088928]

[41]. Singh JA. Risks and benefits of Janus kinase inhibitors in rheumatoid arthritis—past, present, and future. N Engl J Med. 2022;386:387–9. [PubMed: 35081285]

[42]. Brkic S, Stivala S, Santopolo A, Szybinski J, Jungius S, Passweg JR, Tsakiris D, Dirnhofer S, Hutter G, Leonards K, Lischer HEL, Dettmer MS, Neel BG, Levine RL, Meyer SC. Dual targeting of JAK2 and ERK interferes with the myeloproliferative neoplasm clone and enhances therapeutic efficacy. Leukemia. 2021;35:2875–84. [PubMed: 34480104]

[43]. Wolach O, Sellar RS, Martinod K, Cherpokova D, McConkey M, Chappell RJ, Silver AJ, Adams D, Castellano CA, Schneider RK, Padera RF, DeAngelo DJ, Wadleigh M, Steensma DP, Galinsky I, Stone RM, Genovese G, McCarroll SA, Iliadou B, Hultman C, et al. Increased neutrophil extracellular trap formation promotes thrombosis in myeloproliferative neoplasms. Sci Transl Med. 2018;10.

[44]. Gangaraju R, Song J, Kim SJ, Tashi T, Reeves BN, Sundar KM, Thiagarajan P, Prchal JT. Thrombotic, inflammatory, and HIF-regulated genes and thrombosis risk in polycythemia vera and essential thrombocythemia. Blood Adv. 2020;4:1115–30. [PubMed: 32203583]

[45]. Reeves BN, Kim SJ, Song J, Wilson KJ, Henderson MW, Key NS, Pawlinski R, Prchal JT. Tissue factor activity is increased in neutrophils from JAK2 V617F-mutated essential thrombocythemia and polycythemia vera patients. Am J Hematol. 2022;97:E37–40–e40.

[46]. Zhang W, Qi J, Zhao S, Shen W, Dai L, Han W, Huang M, Wang Z, Ruan C, Wu D, Han Y. Clinical significance of circulating microparticles in Ph(−) myeloproliferative neoplasms. Oncol Lett. 2017;14: 2531–6. [PubMed: 28789461]

[47]. Stein BL, McMahon B, Weiss I, Kwaan HC. Tissue-factor bearing microparticles and thrombotic risk in the myeloproliferative neoplasms. Blood. 2012;120:1145.

[48]. Singer JW, Al-Fayoumi S, Taylor J, Velichko S, O'Mahony A. Comparative phenotypic profiling of the JAK2 inhibitors Ruxolitinib, fedratinib, momelotinib, and pacritinib reveals distinct mechanistic signatures. PLOS ONE. 2019;14:e0222944. [PubMed: 31560729]

[49]. Li J, Kent DG, Chen E, Green AR. Mouse models of myeloproliferative neoplasms: JAK of all grades. Dis Model Mech. 2011;4:311–7. [PubMed: 21558064]

[50]. Dunbar A, Nazir A, Levine R. Overview of transgenic mouse models of myeloproliferative neoplasms (MPNs). Curr Protoc Pharmacol. 2017;77:14. 40.1–14.40.19.

[51]. Jacquelin S, Kramer F, Mullally A, Lane SW. Murine models of myelofibrosis. Cancers. 2020;12.

[52]. Matsuura S, Thompson CR, Belghasem ME, Bekendam RH, Piasecki A, Leiva O, Ray A, Italiano J, Yang M, Merill-Skoloff G, Chitalia VC, Flaumenhaft R, Ravid K. Platelet dysfunction and thrombosis in *JAK2*^{V617F}-mutated primary myelofibrotic mice. Arterioscler Thromb Vasc Biol. 2020;40:e262–72. [PubMed: 32814440]

[53]. Grover SP, Mackman N. How useful are ferric chloride models of arterial thrombosis? Platelets. 2020;31:432–8. [PubMed: 31608756]

[54]. Diaz JA, Saha P, Cooley B, Palmer OR, Grover SP, Mackman N, Wakefield TW, Henke PK, Smith A, Lal BK. Choosing a mouse model of venous thrombosis: a consensus assessment of utility and application. J Thromb Haemost. 2019;17:699–707. [PubMed: 30927321]

[55]. Sozer S, Fiel MI, Schiano T, Xu M, Mascarenhas J, Hoffman R. The presence of JAK2V617F mutation in the liver endothelial cells of patients with Budd-Chiari syndrome. Blood. 2009;113:5246–9. [PubMed: 19293426]

[56]. Rosti V, Villani L, Riboni R, Poletto V, Bonetti E, Tozzi L, Bergamaschi G, Catarsi P, Dallera E, Novara F, Massa M, Campanelli R, Fois G, Peruzzi B, Lucioni M, Guglielmelli P, Pancrazzi A, Fiandrino G, Zuffardi O, Magrini U, et al. Spleen endothelial cells from patients with myelofibrosis harbor the JAK2 V617F mutation. Blood. 2013;121:360–8. [PubMed: 23129323]

[57]. Helman R, Pereira WO, Marti LC, Campregher PV, Puga RD, Hamerschlak N, Chiattone CS, Santos FPS. Granulocyte whole exome sequencing and endothelial JAK2V617F in patients with JAK2V617F positive Budd-Chiari syndrome without myeloproliferative neoplasm. Br J Haematol. 2018;180:443–5. [PubMed: 27650062]

[58]. Sharda AV, Bogue T, Barr A, Mendez LM, Flaumenhaft R, Zwicker JI. Circulating protein disulfide isomerase is associated with increased risk of thrombosis in JAK2-mutated myeloproliferative neoplasms. Clin Cancer Res. 2021;27:5708–17. [PubMed: 34400417]

[59]. Teofili L, Martini M, Iachininoto MG, Capodimonti S, Nuzzolo ER, Torti L, Cenci T, Larocca LM, Leone G. Endothelial progenitor cells are clonal and exhibit the JAK2V617F mutation in a subset of thrombotic patients with Ph-negative myeloproliferative neoplasms. Blood. 2011;117:2700–7. [PubMed: 21212285]

[60]. Piaggio G, Rosti V, Corselli M, Bertolotti F, Bergamaschi G, Pozzi S, Imperiale D, Chiavarina B, Bonetti E, Novara F, Sessarego M, Villani L, Garuti A, Massa M, Ghio R, Campanelli R, Bacigalupo A, Pecci A, Viarengo G, Zuffardi O, et al. Endothelial colony-forming cells from patients with chronic myeloproliferative disorders lack the disease-specific molecular clonality marker. Blood. 2009;114: 3127–30. [PubMed: 19628707]

[61]. Sano S, Wang Y, Yura Y, Sano M, Oshima K, Yang Y, Katanasaka Y, Min KD, Matsuura S, Ravid K, Mohi G, Walsh K. JAK2 (V617F)-mediated clonal hematopoiesis accelerates pathological remodeling in murine heart failure. JACC Basic Transl Sci. 2019;4:684–97. [PubMed: 31709318]

[62]. Tripodo C, Burocchi A, Piccaluga PP, Chiodoni C, Portararo P, Cappetti B, Botti L, Gulino A, Isidori A, Liso A, Visani G, Martelli MP, Falini B, Pandolfi PP, Colombo MP, Sangaletti S. Persistent immune stimulation exacerbates genetically driven myeloproliferative disorders via stromal remodeling. Cancer Res. 2017;77:3685–99. [PubMed: 28536276]

Essentials

- Several janus kinase (JAK)-signal transducer and activator of transcription (STAT) inhibitors are known to increase thrombosis risk.
- It is unknown whether JAK-STAT inhibitors increase vascular activation.
- JAK-STAT inhibition with ruxolitinib and fedratinib reduced proadhesive, proinflammatory, and procoagulant activation.
- JAK-STAT inhibitor prevents rolling and adhesion of normal and *JAK2*$^{V617F+}$ blood on activated endothelium.

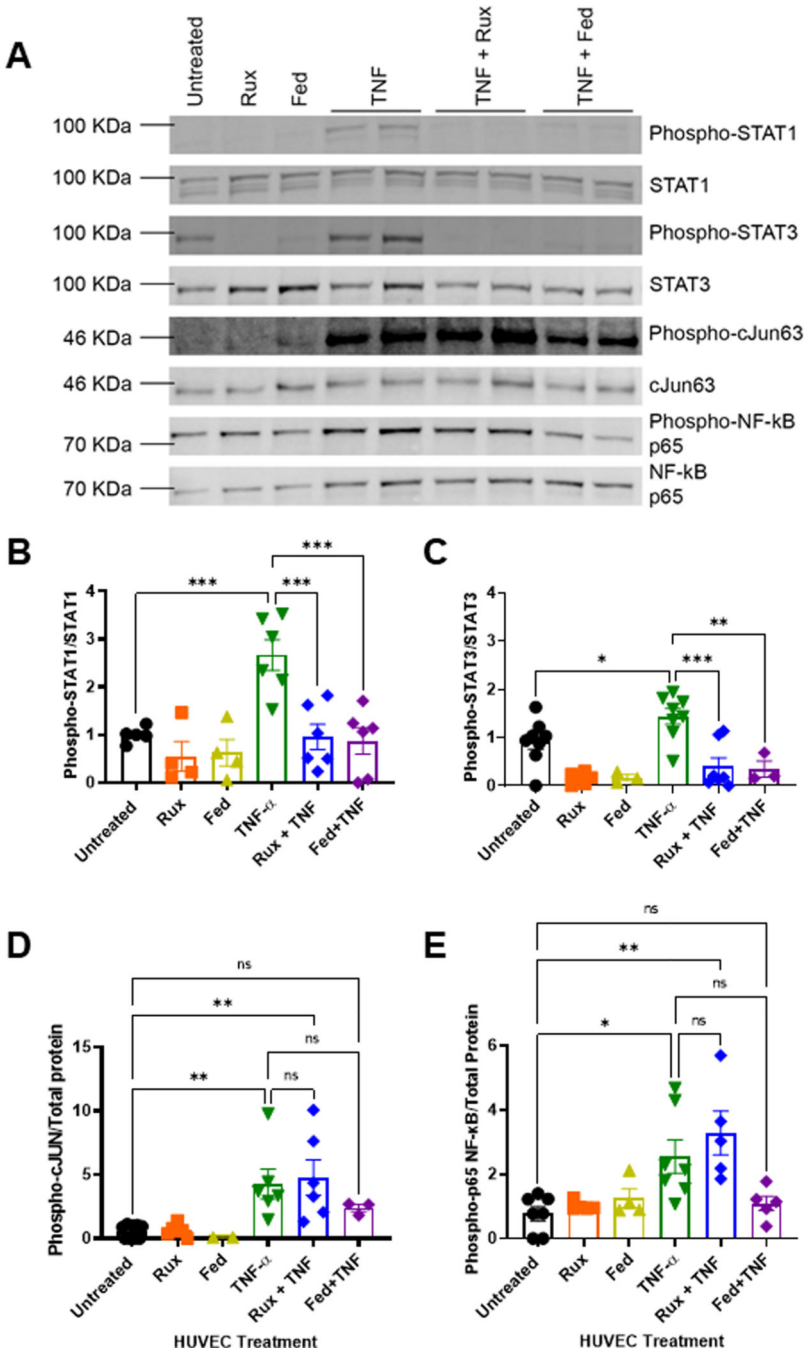

FIGURE 1.

Ruxolitinib and fedratinib inhibit TNF-α-mediated STAT1 and STAT3 with attenuation of c-Jun and NF-κB. A. Representative western blots of nuclear lysates from human umbilical vein endothelial cells (HUVEC) treated with 0.4 μM ruxolitinib or 1 μM fedratinib JDB for 30 minutes followed by addition of 10 ng/mL TNF-α for 4 hours. Nuclear extracts collected and separated on 10% Tris-Hcl gel, transferred to PVDF membrane, and followed by total protein stain and immunoprobes against phospho-antibodies. Membranes were stripped and re-probed for unphosphorylated forms. B. Densitometry values from 5 different westerns

blots probed for phospho-STAT1 normalized to total STAT1. C. Densitometry values from 5 different western blots for phospho-STAT3 normalized to total STAT3. D. Densitometry values for 5 different westerns blots probed for phospho-C-JUN normalized to total protein values. E. Densitometry values for 5 different western blots probed for phospho-p65 NF-κB to total protein. Error bars represent mean ±SE of means. *p* values from analysis of variance testing with appropriate post-hoc multiple comparison testing. ns, not significant. * $p < .05$, ** $p < .01$, *** $p < .001$.

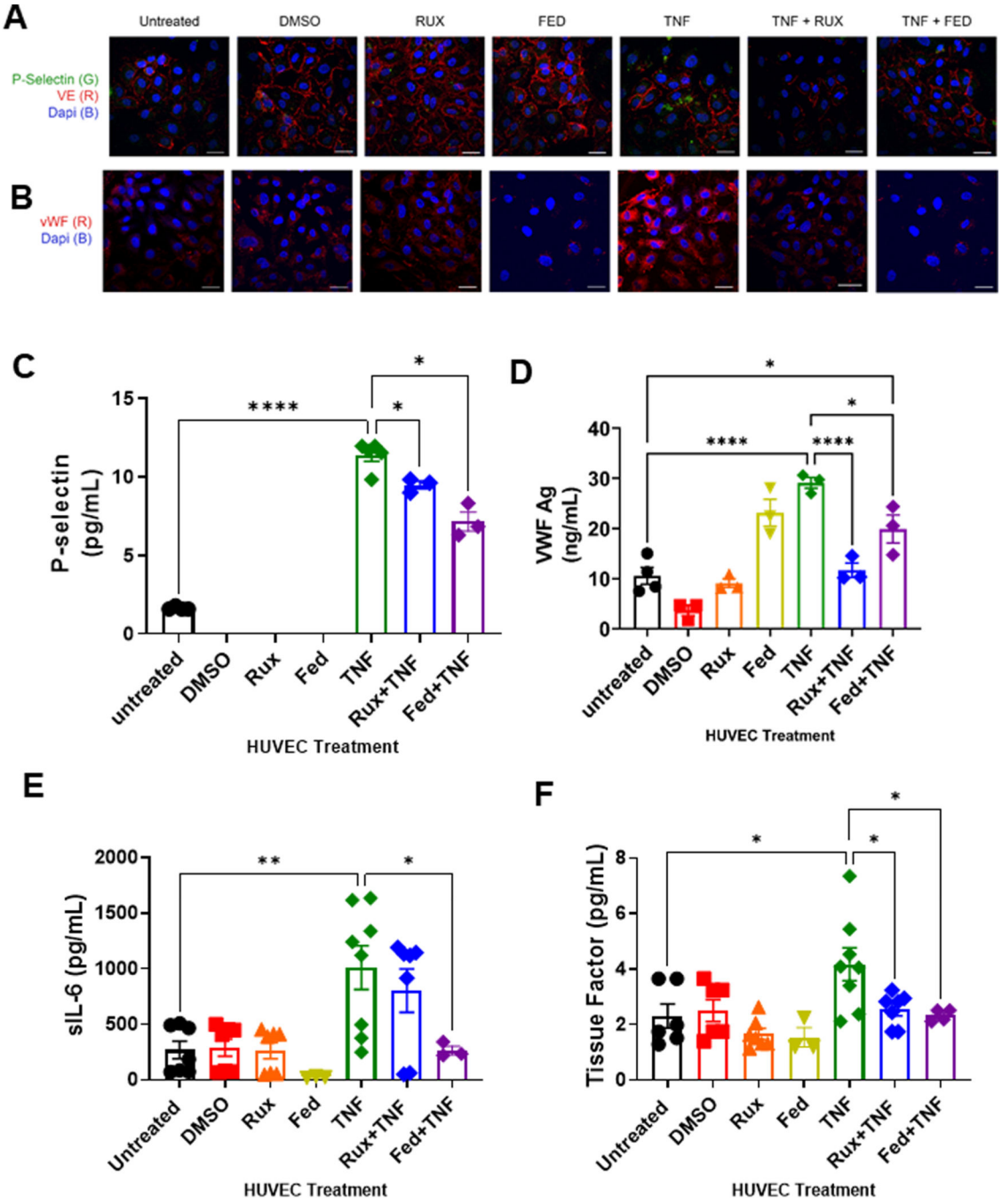

FIGURE 2.

Ruxolitinib and fedratinib decrease TNF-α mediated release of P-selectin and VWF and reduce secretion of IL-6 and tissue factor. HUVEC were treated with 0.4 μM ruxolitinib or 1 μM fedratinib JDB for 30 minutes followed by addition of 10 ng/mL TNF-α for 4 hours. Conditioned media was collected for ELISA. Cells were fixed and stained for the following analyses. (A) Confocal microscopy demonstrating release of P-selectin from endothelial cells. Unpermeablized HUVEC were stained for P-selectin (green) and VE-cadherin (red) and nuclei counterstained with DAPI. (B) Confocal microscopy demonstrating surface

expression of VWF. Unpermeablized HUVEC were stained for VWF (red) and nuclei counterstained with DAPI. (C) ELISA assay for soluble P-selectin (sP-selectin). (D) ELISA assay for sVWF antigen. (E) Cytokine array results for sIL-6. (F) Cytokine arrays results for tissue factor. Each dot represents an individual replicate from a total of 3 separate experiments, with $n = 2$ to 3 replicates per experiment. For sP-selectin, VWF, and sIL-6, several replicates had undetectable levels. Error bars represent mean ±SE of means. p values from analysis of variance testing with appropriate post-hoc multiple comparison testing. ns, not significant. * $p < .05$, ** $p < .01$, *** $p < .001$, **** $p < .0001$.

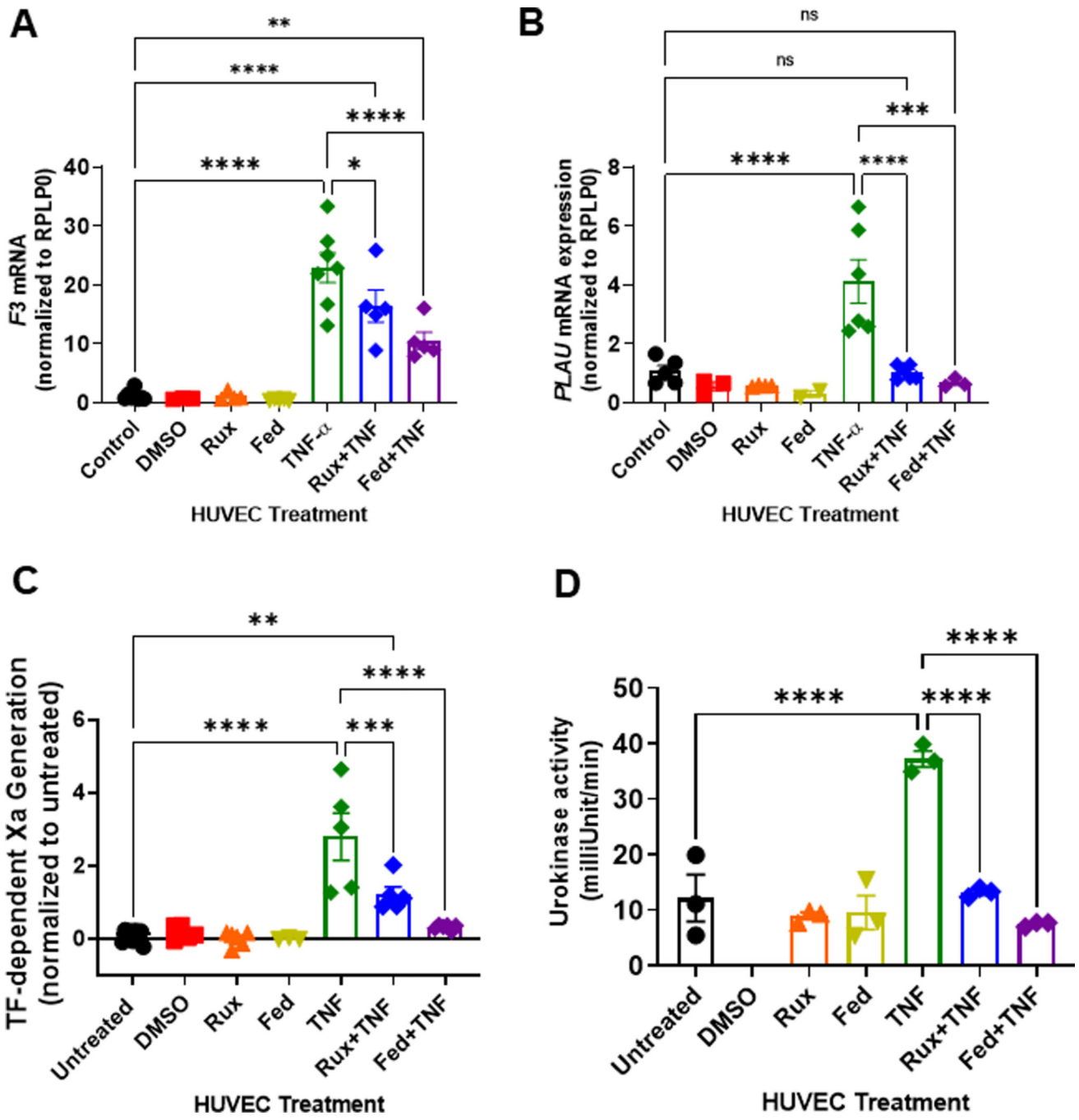

FIGURE 3.

Ruxolitinib and fedratinib decrease TNF-α mediated tissue factor and urokinase mRNA upregulation and decrease tissue factor and urokinase activity. HUVEC were treated with 0.4 μM ruxolitinib or 1 μM fedratinib JDB for 30 minutes followed by addition of 10 ng/mL TNF-α for 4 hours. (A) Tissue factor (Factor 3, F3) mRNA levels were normalized to control. (B) Plasminogen activator urokinase (PLAU) mRNA levels were normalized to control. For activity assays, HUVEC were treated with 0.4 μM ruxolitinib or 1 μM fedratinib for 30 minutes followed by addition of 10 ng/mL TNF-α for 4 hours JDB.

(C). Measurement of tissue factor (TF)-dependent Xa generation was performed using Chromagenix Xa solution as described in methods. Results are normalized to untreated cells. (D). For urokinase activity, conditioned media were collected followed by urokinase activity measurement (Abcam). For all graphs, each dot represents an individual replicate from $n = 2$ to3 separate experiments. Error bars represent mean ±SE of means. p values from analysis of variance testing with appropriate post-hoc multiple comparison testing. ns, not significant. * $p < .05$, ** $p < .01$, *** $p < .001$, **** $p < .0001$.

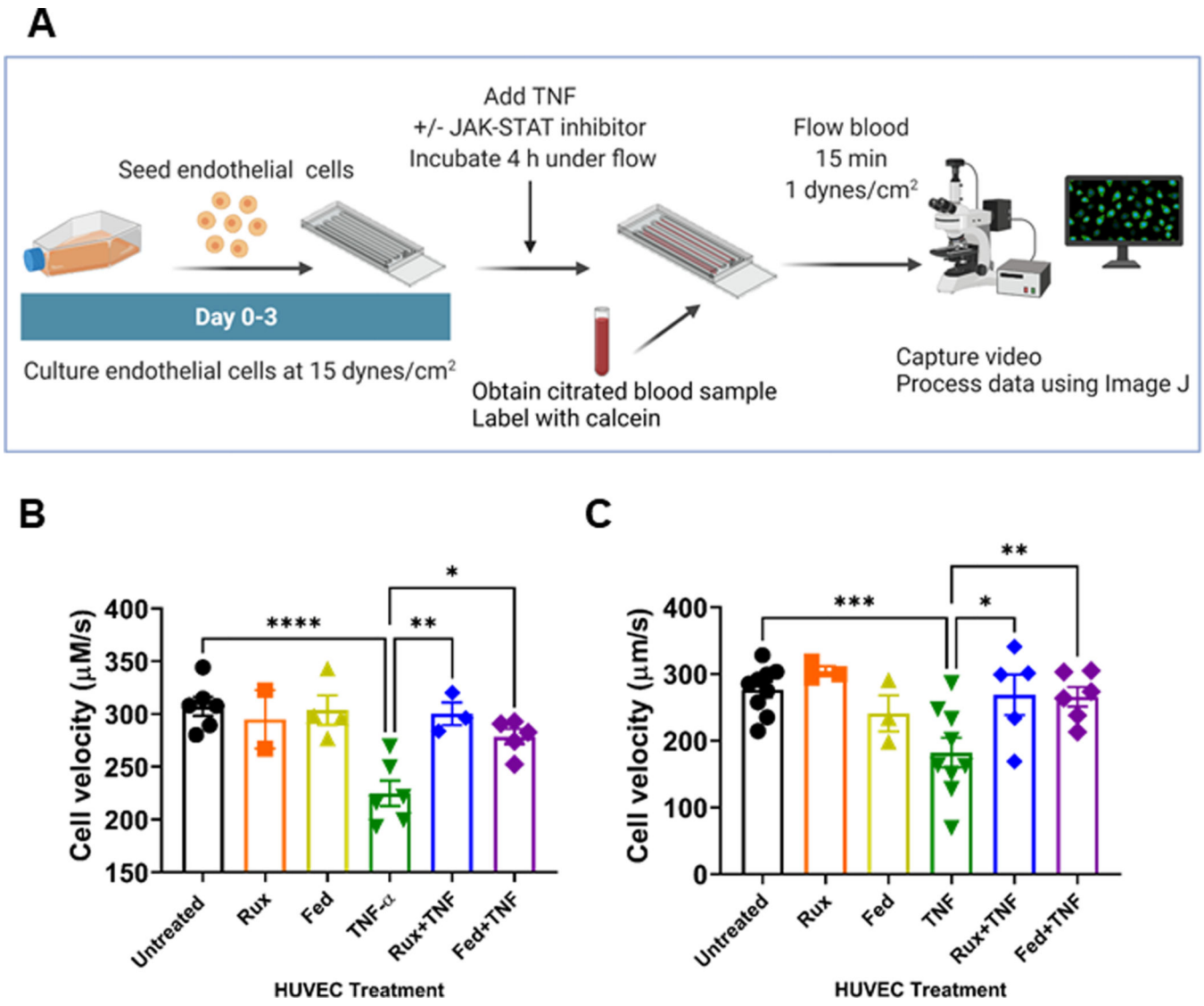

FIGURE 4.

Treatment of endothelium with ruxolitinib or fedratinib prevents TNF-α mediated cell velocity reduction at venous shear rate. A. Experimental schematic for endotheliazed devices and approach to evaluate effects on endothelial activation. HUVEC were cultured under flow for 3 days at 15 dynes/cm^2. Endothelialized devices were then treated with ± 10 ng/mL TNF-α and/or ± 0.4 μM ruxolitinib or 1 μM fedratinib for 4 hours. Whole blood from donors was collected in sodium citrated and labeled with calcein. Whole blood was then perfused over endothelial cells for 15 minutes at 1 dynes/cm^2. Image created in BioRender.com B. Cell velocity of calcein+ cells obtained from control blood donors (n = 7 donors with n = 3 to 7 replicates per conditions. C. Cell velocity of calcein+ cells obtained from *JAK2*$^{V617F+}$ (n = 9 donors with n = 3 to 9 replicates per condition, red) blood donors. All data ±SE of means. p values from one-way repeated measure ANOVA with Holm–Sidak's multiple comparisons test. * $p < .05$, ** $p < .01$, *** $p < .001$, **** $p < .0001$.

TABLE 1

Characteristics of whole blood donors.

Parameter	Controls (n = 7)	*JAK2*V617F+ (n = 9)	95% CI of the difference[b]		p value
Age	32 (range 18–62)	58 (range 25–79)	NA		NA
Sex					
Male	5	3	NA		**NA**
Female	2	6			
Ethnicity					
White	3	7	NA		**NA**
Non-White	4	2			
Complete blood count parameters[a]					
White blood cells (10^7/dL)	7.3 ± 0.8	8.3 ± 1.1	−2.0	4.11	.5
Hemoglobin (g/dL)	13.6 ± 0.3	13.3 ± 0.5	−1.7	1.2	.7
Hematocrit (%)	**37.4 ± 1.1**	**42.8 ± 1.8**	**0.5**	**10.2**	**.03**
Platelet (10^7/dL) [c]	**238 ± 38**	**602 ± 168**	**8.8**	**786**	**.05**
Thrombosis history (n, %)	NA	**2 (33.3%)**	NA		
Phenotype[d]	NA		NA		
Essential thrombocythemia		1			
Polycythemia vera		7			
Myelofibrosis		1			
Medications	NA		NA		
Aspirin		6			
Hydroxyurea		4			
Interferon		0			
Ruxolitinib		0			

[a] values mean ± SM of means.

[b] CIs and p value from unpaired t-test.

[c] t-test with Welch's correction for unequal SDs used.

[d] Phenotype based on electronic medical record, laboratory values, and bone marrow at the time of diagnosis. Bold values indicate values with significant trends or differences.